Entanglement growth and simulation efficiency in one-dimensional quantum lattice systems

Álvaro Perales[1,2] and Guifré Vidal[2]
[1]*Departamento Automática, Universidad de Alcalá, Alcalá de Henares, Madrid 28871, Spain*
[2]*School of Physical Sciences, The University of Queensland, QLD 4072, Australia*
(Received 23 November 2007; revised manuscript received 27 June 2008; published 31 October 2008)

We study the evolution of one-dimensional quantum lattice systems when the ground state is perturbed by altering one site in the middle of the chain. For a large class of models, we observe a similar pattern of entanglement growth during the evolution, characterized by a moderate increase of significant Schmidt coefficients in all relevant bipartite decompositions of the state. As a result, the evolution can be accurately described by a *matrix product state* and efficiently simulated using the *time-evolving block decimation* algorithm.

DOI: 10.1103/PhysRevA.78.042337 PACS number(s): 03.67.Bg, 75.10.Pq, 03.67.Ac, 05.50.+q

I. INTRODUCTION

The numerical study of quantum many-body systems is a challenging computational task due to the exponential growth of the Hilbert space dimension with the system's size. Lattice systems in one spatial dimension, such as quantum spin chains, are a noticeable exception. There, the density matrix renormalization group (DMRG) algorithm allows for the precise computation of ground state properties [1], while the time-evolving block decimation (TEBD) algorithm can be used to simulate time evolution [2,3]. Such techniques provide valuable insight into quantum systems, therefore facilitating progress in several forefront areas of research, both in science—e.g., condensed matter, quantum optics, atomic and nuclear physics, quantum chemistry—and technology—e.g., quantum information processing, quantum computation, nanotechnology.

Many-body entanglement is at the very core of the achievements of the DMRG and TEBD algorithms. In both cases, a key ingredient is the use of a matrix product state (MPS) to represent the state $|\Psi\rangle$ of the system [4]. A MPS leads to an *efficient* representation of $|\Psi\rangle$ provided that the amount of entanglement in the system is sufficiently small. Thus the success of the DMRG relies on the remarkable fact that in one spatial dimension the ground state of most local Hamiltonians has only a limited amount of entanglement. Likewise, the TEBD algorithm, based on updating the MPS in time, is efficient as long as no large amounts of entanglement are produced during the simulated evolution.

Identifying time evolutions that only involve small amounts of entanglement is, consequently, of central importance in order to establish the range of applicability of the TEBD algorithm—and of a whole score of subsequent proposals [5–8], including implementations within the DMRG formalism [6–8] often referred to as tDMRG, that are based on the same idea, namely on adapting the MPS representation of the state of the system, so as to account for its changes during a time evolution. At the same time, a better understanding of the dynamics of entanglement in one-dimensional many-body systems [9] is of interest in the areas of quantum-information processing, where entanglement is regarded as a useful resource, and of quantum computation, where entanglement is necessary in order to achieve a significant speed-up with respect to classical computers [2,10].

In this paper we study the generation of entanglement in a particularly relevant class of time evolutions. Specifically, we consider a chain of N sites, where each site is represented by a finite-dimensional Hilbert space and labeled by s ($s=1,\ldots,N$). The system, initially prepared in the ground state $|\Psi_{\mathrm{GS}}\rangle$ of some local Hamiltonian H, is perturbed at time $t=0$ by applying an operator A on lattice site s_0. As a result, the state of the system $|\Psi(0)\rangle \equiv A^{s_0}|\Psi_{\mathrm{GS}}\rangle$, no longer an eigenstate of H, evolves nontrivially in time, see, e.g., Fig. 1,

$$|\Psi(t)\rangle \equiv e^{-iHt}|\Psi(0)\rangle = e^{-iHt}A^{s_0}|\Psi_{\mathrm{GS}}\rangle. \tag{1}$$

During this evolution entanglement is produced, adding to the entanglement that might already be present in the ground state.

Notice that state $|\Psi(t)\rangle$ appears in the computation of the unequal time correlation function

$$\begin{aligned}\langle B^s(t)A^{s_0}(0)\rangle &\equiv \langle\Psi_{\mathrm{GS}}|e^{iHt}B^s e^{-iHt}A^{s_0}|\Psi_{\mathrm{GS}}\rangle \\ &= e^{iE_0 t}\langle\Psi_{\mathrm{GS}}|B^s|\Psi(t)\rangle,\end{aligned} \tag{2}$$

where a second operator B has been applied on site s at time t. Therefore, by characterizing the growth of entanglement in evolution (1), we will be able to assess the efficiency with which the algorithms of Refs. [2,3,5–8] can be used to compute the two-point correlator (2). We recall that from this correlator one can extract quantities such as Green's functions or dynamic structure factors, and thus learn about a number of properties of the system, including its response to external probes, e.g., neutron or photon scattering.

The study of the entanglement and stimulability of a time evolution of the form (1) was initiated in Ref. [3] and is intimately related to the development of the TEBD algorithm. Originally, the TEBD algorithm was created in order to characterize the role of entanglement in quantum computation [2]. Soon afterward it was noticed that, for systems in one spatial dimension, low energy time evolutions such as Eq. (1) seemed to often involve small amounts of entanglement [3], precisely in the way that would allow the TEBD algorithm to work efficiently. This opened up the possibility to simulate this class of dynamics. One may claim, *a posteriori*, that it is somehow expected that no such entanglement will be created when a single local perturbation is introduced on the ground state $|\Psi_{\mathrm{GS}}\rangle$ of H. However, the subject is far from being well-understood and, for instance, given H and local operator A, there are no known conditions to guarantee that the evolution can be simulated efficiently for reasonably

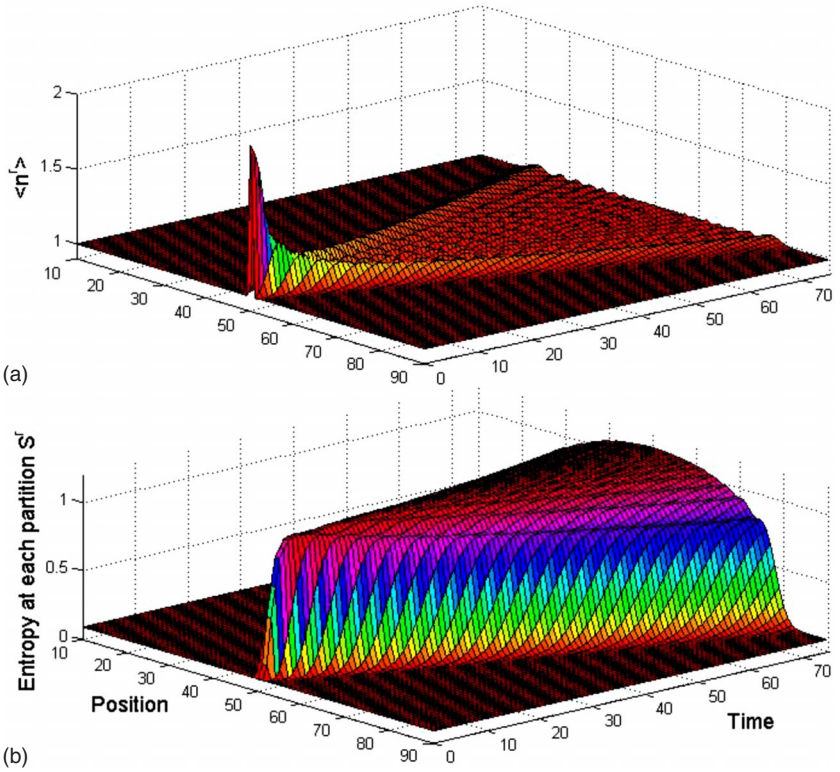

FIG. 1. (Color online) Propagation of a perturbation introduced in the middle of a chain of $N=100$ sites. This evolution corresponds to a Bose-Hubbard model, Eq. (9), in the Mott-insulating phase (hopping term $J=0.1$, on-site repulsion $U=1$, and chemical potential $\mu=0.5$) with one boson per site. (a) Expectation value $\langle n^r \rangle$ for the number operator on each site, as a function of time, after an extra boson is introduced on site $s_0=50$. The perturbation propagates throughout the chain, occupying a region that grows linearly in time until reaching the boundaries. (b) The entanglement entropy S^r shows how every bipartition remains almost disentangled until the arrival of the wave front. When the front has gone far away, the entropy saturates.

long times. The best result in this direction, due to Osborne [11], shows that time evolutions in one spatial dimension can be simulated efficiently (that is, with polynomial resources in N) only up to small times $t \approx \log(N)$. Instead, numerics suggest that the simulation of Eq. (1) can be performed efficiently for times that scale at least as the size of the system, $t \approx N$ [3,8].

Several authors (see, for instance, [3,6,12–15]) have already considered particular instances of evolution ensuing either a *local perturbation* of the ground state as in Eq. (1), or a *local quench* (which is qualitatively equivalent to a local perturbation). In these specific cases it has been observed that, indeed, the amount of entanglement remains sufficiently small as to allow practical simulations for large times and system sizes (in a sense further specified in the next section). The goal of the present paper is to establish how general this result is by conducting a systematic numerical study of evolutions of the form (1) in one-dimensional models, including: (i) systems of spins, fermions, and bosons; (ii) gapped and gapless phases; (iii) homogeneous and disordered interactions; and (iv) integrable and nonintegrable systems. We find that, whereas for each model the evolution may represent a very different physical process, in all cases the dynamics of entanglement, remarkably similar, are characterized by a moderate growth. As a result, the evolution can be simulated, with reasonably modest computational resources, for times long enough that the perturbation, initially localized, can spread over large regions, involving, e.g., of the order of 100 sites.

We notice that the TEBD algorithm has also been applied to other classes of evolution. In the case of a *global quench* that modifies the Hamiltonian everywhere in the chain, or when the initial state of the system does belong to the low energy sector of H, it has been reported that a large amount of entanglement is created [16,17] and therefore the simulation becomes inefficient. We emphasize that this is not at all surprising, given the exponentially large dimension of the Hilbert space in the system size, which implies that a generic state of the system cannot be represented efficiently. Instead, what is truly remarkable (and useful for practical simulations) is that there are circumstances of interest where the state of the system can be efficiently encoded using a MPS. Apart from the case of a local perturbation of the ground state (local quench), there are not many other classes of evolution known that can be efficiently simulated for reasonably large times. One noticeable exception is the case of a global quench in a *disordered system* [17], which seems to be related to localization effects experienced by information in the presence of disorder [18]. Another case, perhaps less surprising but still potentially very useful, is the evolution of observables and of thermal states after a global quench in *integrable* systems [19].

The rest of the paper is organized as follows. In Sec. II we introduce the measure of entanglement that is relevant in the present context and describe the one-dimensional models we have considered. In Sec. III we present the results of the simulations. Specifically, we describe two cases that illustrate the two types of scaling of entanglement observed in all the simulations we have performed. In Sec. IV we discuss the previous results, including simple toy models that reproduce the entanglement scaling reported in Sec. III and present some conclusions.

II. ENTANGLEMENT MEASURE AND ONE-DIMENSIONAL MODELS

Our goal is to characterize the growth of entanglement during the time evolution that takes place after the ground

state $|\Psi_{\mathrm{GS}}\rangle$ of a one-dimensional (1D) system has been perturbed by some local operator A, Eq. (1). In the present context, an appropriate measure of the entanglement contained in $|\Psi(t)\rangle$ is provided by the number χ of terms in its Schmidt decompositions (we refer to [2,3] for details). More specifically, given a partition of the chain into two blocks containing the first r sites and the remaining $N-r$ sites, respectively, the Schmidt decomposition reads

$$|\Psi(t)\rangle = \sum_{\alpha=1}^{\chi^r} \lambda_\alpha^r |\Phi_\alpha^{1:r}\rangle |\Phi_\alpha^{r+1:N}\rangle, \tag{3}$$

where the rank χ^r, the Schmidt coefficients λ_α^r, and the Schmidt bases $|\Phi_\alpha^{1:r}\rangle$ and $|\Phi_\alpha^{r+1:N}\rangle$ are all time dependent. Equation (3) contains in principle a very large number of terms, with $\chi^r \sim \exp(N)$. However, when the Schmidt coefficients λ_α^r decay fast with α, a good approximation to $|\Psi(t)\rangle$ may be obtained by keeping only a relatively small number χ_ϵ^r of terms. The truncation introduces a small error ϵ [20], given by

$$\epsilon \equiv 1 - \sum_{\alpha=1}^{\chi_\epsilon^r} (\lambda_\alpha^r)^2. \tag{4}$$

The exact and approximate ranks χ and χ_ϵ of $|\Psi(t)\rangle$ are then defined by maximizing over bipartitions,

$$\chi \equiv \max_r \chi^r, \quad \chi_\epsilon \equiv \max_r \chi_\epsilon^r. \tag{5}$$

A MPS can store the truncated state using $O(N\chi_\epsilon^2)$ coefficients, while the cost of simulating a time step scales as $O(N\chi_\epsilon^3)$. Therefore χ_ϵ is indicative of the computational resources required in an approximate simulation with truncation error ϵ. Although in an actual simulation there might be other sources of errors, such as those due to Trotter expansion [3], and errors accumulate in time, the simple entanglement measure χ_ϵ turns out to be informative enough as to allow us to assess in practice whether a simulation is efficient.

We have considered a large number of quantum models on a one-dimensional lattice. Our hope is that by studying these models, we already observe all possible forms of scaling of entanglement, as measured by χ_ϵ, so that we can draw conclusions that are valid for generic 1D systems—or at least for those 1D systems that are usually of interest in condensed matter physics and quantum statistical mechanics. The specific models we have considered are as follows.

(1) The quantum Ising model with parallel and transverse magnetic fields

$$H_{\mathrm{Ising}} = \sum_r \sigma_x^r \sigma_x^{r+1} + \sum_r (h_x \sigma_x^r + h_z \sigma_z^r), \tag{6}$$

where h_x and h_y are the intensity of uniform magnetic fields in the x (parallel) and z (perpendicular) directions. For $h_x=0$, a Jordan-Wigner transformation maps this quantum spin model (with spin $\frac{1}{2}$) into a model of free spinless fermions.

(2) The quantum XY model with transverse magnetic field

$$H_{XY} = \sum_r \left(\frac{1+\gamma}{2} \sigma_x^r \sigma_x^{r+1} + \frac{1-\gamma}{2} \sigma_y^r \sigma_y^{r+1} + h_z^r \sigma_z^r \right), \tag{7}$$

where γ is the anisotropy parameter and h_z^r the intensity of a (possibly site-dependent) transverse magnetic field. For $\gamma=1$ we recover the quantum Ising model with transverse magnetic field, whereas $\gamma=0$ corresponds to the quantum XX model, which is also used as a model of hard-core bosons. Again, a Jordan-Wigner transformation maps this quantum spin model (with spin $\frac{1}{2}$) into a model of free spinless fermions.

(3) The quantum XXZ model with magnetic field in the z direction

$$H_{XXZ} = \sum_r (\sigma_x^r \sigma_x^{r+1} + \sigma_y^r \sigma_y^{r+1} + \Delta \sigma_z^r \sigma_z^{r+1} + h_z^r \sigma_z^r), \tag{8}$$

where Δ is the anisotropy parameter and h_z^r the intensity of a (possibly site-dependent) magnetic field in the z direction. For $\Delta=0$ we recover the XX model, for $\Delta=1$ a spin-$\frac{1}{2}$ Heisenberg quantum antiferromagnet and for $\Delta=-1$ a model locally equivalent to a spin-$\frac{1}{2}$ Heisenberg quantum ferromagnet. Through a Jordan-Wigner transformation H_{XXZ} becomes a model of interacting spinless fermions.

(4) The Bose-Hubbard model

$$H_{\mathrm{BH}} = \sum_s [-J(b^{\dagger s} b^{s+1} + \mathrm{H.c.}) - \mu n^s + U n^s (n^s - 1)], \tag{9}$$

a model of interacting bosons where J is the hopping amplitude; μ is the chemical potential, U is the on-site repulsion; and $b^{\dagger s}$, b^s, and $n^s = b^{\dagger s} b^s$ are the bosonic creation, annihilation, and number operators at site s, respectively.

For all the above models we have considered gapped and gapless cases. For the XY and XXZ models we have considered, in addition to uniformed magnetic fields, disordered versions by introducing inhomogeneous, random magnetic fields h_z^r.

III. RESULTS

We have simulated time evolutions of the form (1) for each of the variants of the models (6)–(9) of the previous section for chains with open boundary conditions and with a number N ranging from 100 to 200. After computing the ground state $|\Psi_{\mathrm{GS}}\rangle$ of a given Hamiltonian H through a simulation of imaginary time evolution [3], at $t=0$ an operator A is applied to the middle of the chain. The system is then allowed to evolve according to the time evolution operator e^{-iHt}, which results in a propagation of the perturbation from the center of the chain toward its ends. We stop the simulations before the signal reaches the boundary of the chain. Chains of different lengths have been simulated in order to guarantee that our results are essentially independent of the system's size. Convergence of the results in this sense is only possible in those models where the correlation length is sufficiently smaller than the system's size. We notice that systems at or very close to a quantum critical point fail to fulfill this condition. Also, the simulations have been performed with a MPS of rank χ^* much larger than the reported χ_ϵ, in

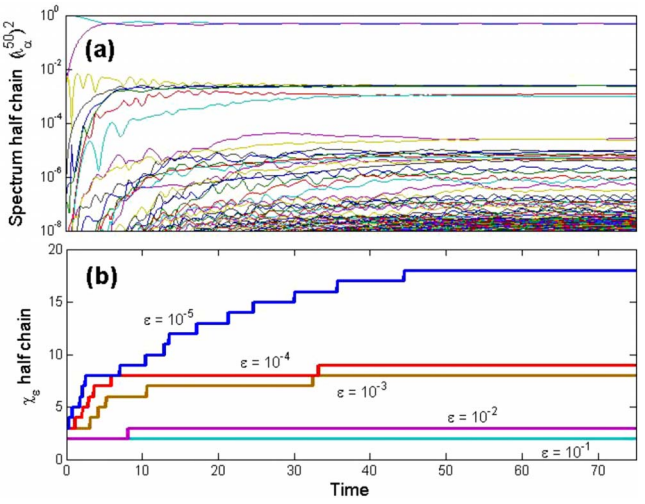

FIG. 2. (Color online) Entanglement growth at the center of the chain for the Bose-Hubbard model, Eq. (9), in the same scenario as Fig. 1. (a) Starting from a barely entangled state, with only a few nonvanishing Schmidt coefficients, several other coefficients start to grow, then saturate. (b) The approximate rank χ_ϵ first grows, then saturates at a number that increases as we decrease the truncation error ϵ. This implies that an accurate approximation to $|\Psi(t)\rangle$ can be stored in a MPS with a small rank χ_ϵ that after some time becomes roughly constant.

order to guarantee that our analysis is independent of the computational resources devoted to the numerical simulation used to obtain them. Specifically, we report results for $\chi_\epsilon \leqslant 35$ which have been obtained by simulating the evolution with a MPS with $\chi^*=80$, 100, and 150.

The evolution in all simulations has been carried out with a fourth-order Trotter expansion (labeled as $\mathcal{Z}_4^1$ in [22]) with a time step $\delta t=0.02$. The associated Trotter error is $\epsilon_{\text{Trott}} \propto \delta t^5 T/\delta t = 8\times 10^{-6}$ for $T=50$ time units. The computation times varied from a few hours to 3 weeks in the worst case, in a PC with a dual core processor at 2.2 GHz with 4 GB of RAM. In the Bose-Hubbard model, each site was truncated to four levels.

We observe that, in spite of the rather diverse nature of the physics described by the models (6)–(9), the scaling of its entanglement in time follows a very similar pattern. Next we describe in detail the results obtained for two specific systems. They have been chosen as representatives of the behavior of χ_ϵ in all the models under study.

Example I: Saturation. Our first example is concerned with a system of interacting bosons described by the Bose-Hubbard model H_{BH} of Eq. (9) in a chain with $N=100$ sites. Figure 1(a) shows the reorganization of the density of bosons when one extra particle is introduced in the middle of the chain, which is in the Mott insulating phase. Figure 2(a) presents the changes in the spectrum of the squared Schmidt coefficients $(\lambda_\alpha^{r=50})^2$ during the evolution. We depict the Schmidt coefficients for $r=50$ (middle of the chain) because this is the bipartition that appears most entangled (i.e., $\chi_\epsilon = \chi_\epsilon^{r=50}$ for all ϵ) at all times (except some minor corrections of one or two sites). We measure time in $1/U$ units, and choose $U=1$.

We notice that there are two marked regimes. First, for times up to $t=20-30$, a number of Schmidt coefficients increase monotonically, with a growth that progressively slows down. Bipartite entanglement between the left and the right halves of the chain is being created (see an analogous behavior obtained analytically in Ref. [15]). Then, for larger times, and coinciding with the fact that the fronts of the density wave are far from the middle of the chain, the Schmidt coefficients become roughly stationary, indicating that the production of bipartite entanglement at the center of the chain has come to a halt. Notice that this is reflected in an initial growth, then saturation, of χ_ϵ, as depicted in Fig. 2(b). Elsewhere in the chain, say $r=30$, no bipartite entanglement is generated until the front of the density wave arrives. At that point, the Schmidt coefficients λ_α^{30} start increasing to later become stationary, in a pattern that mimics what occurred at the center of the chain, but with increasingly delayed and attenuated growth as we move away from the center. The entanglement entropy of a bipartition,

$$S^r \equiv -\sum_\alpha (\lambda_\alpha^r)^2 \log_2(\lambda_\alpha^r)^2, \tag{10}$$

offers a complementary, coarse-grained picture into the entanglement growth in the system that confirms the above observations; see Fig. 1(b).

Example II: Moderate steady growth. A slightly different pattern of entanglement growth occurs in the antiferromagnetic quantum Ising model with tilted magnetic field H_{Ising} of Eq. (6) with $N=200$ spins. Figure 3(a) shows the propagation of a magnetization wave produced by flipping one spin in the center of the chain, $r=100$, for the case $h_x=h_z=1$. Figure 4(a) shows that, as in the first example, a number of Schmidt coefficients first grow substantially and then tend to saturate. An important difference, however, is revealed by studying χ_ϵ, Fig. 4(b). For $\epsilon=0.1, 0.01$, the approximate rank χ_ϵ again saturates, but for smaller ϵ it keeps growing in time. This is due to the appearance of an increasingly large number of small Schmidt coefficients that need to be considered collectively in order to decrease the truncation error ϵ. Although it is difficult to characterize the scaling of χ_ϵ in time, we obtain results compatible with $\chi_\epsilon \sim t^p$ for a power p of the order of 1. Correspondingly, a plot of the entropy, Fig. 3(b), shows an initial rapid growth followed by a much slower, possibly logarithmic growth at longer times.

IV. DISCUSSION

Our simulations show a strikingly similar pattern of entanglement generation in all the systems we have studied [21]. In particular, we always find a sufficiently large ϵ, e.g., $\epsilon=10^{-2}$ in the examples of the previous section, for which χ_ϵ seems to saturate as a function of time. This means that a MPS with fixed rank χ_ϵ already suffices to approximate (to accuracy ϵ) the state of the chain during the *whole* evolution. However, if we now try to improve this accuracy by lowering ϵ, we find two possible behaviors. In some cases, as in example I, the rank $\chi_{\epsilon=10^{-3}}$ still saturates, although at a later time. In some other cases, as in example II, $\chi_{\epsilon=10^{-3}}$ keeps growing indefinitely (that is, as far as we could see with our computational resources), with a shape that resembles a small power of time $\chi_\epsilon \sim t^p$. This moderate entanglement

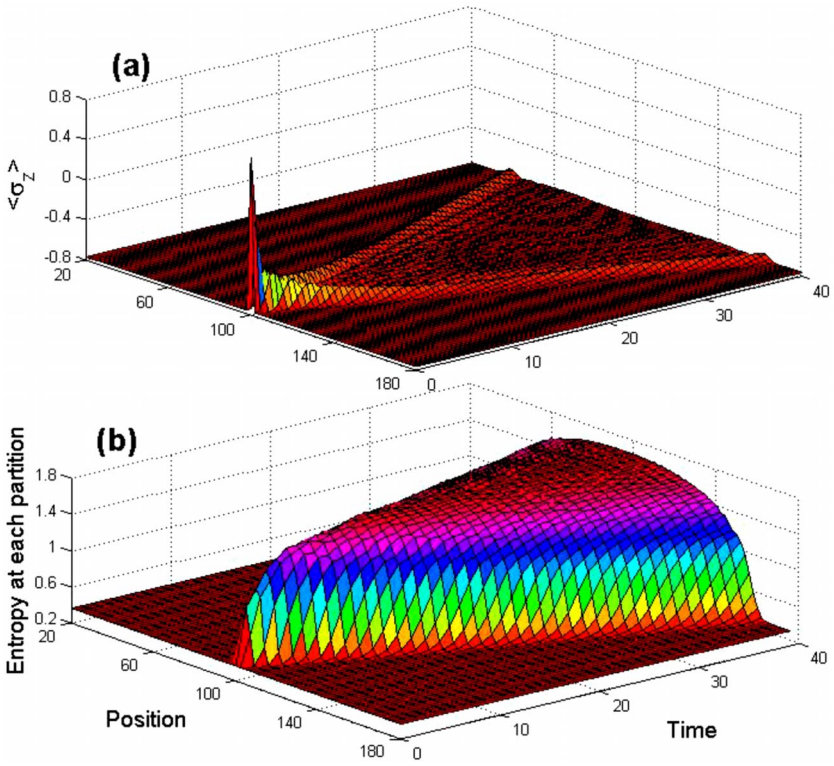

FIG. 3. (Color online) Propagation of a perturbation introduced in the middle of a chain with $N=200$ sites, corresponding to the Ising model with tilted magnetic field, Eq. (6), with $h_x=h_z=1$. Starting with a slightly entangled ground state, at $t=0$ one spin is flipped on site 100 applying $\sigma_x^{r=100}$. The evolution of both (a) the expectation value $\langle\sigma_z^r\rangle$ for the magnetization on the z direction and (b) the entropy of a bipartition resemble their analogs in the Bose-Hubbard model, Fig. 1. However, Fig. 4 reveals that more entanglement is generated in this second system.

growth agrees with the analytical result obtained in Ref. [12] in a similar scenario. By means of conformal field theory they show that the entropy grows logarithmically with time, $S(t)\sim\log(t)$, when two initially decoupled quantum chains are joined together. This corresponds as well to a local quench of the ground state, and the subsequent evolution is expected to be analogous in terms of entanglement creation through the whole chain. These mild behaviors are in sharp contrast with the exponential growth, $\chi_\epsilon\sim e^t$, that one finds, e.g., in a spin model where at time $t=0$ the value of the magnetic field throughout the whole chain is changed (global quench) or the spins in half of the chain are flipped [12,16,17].

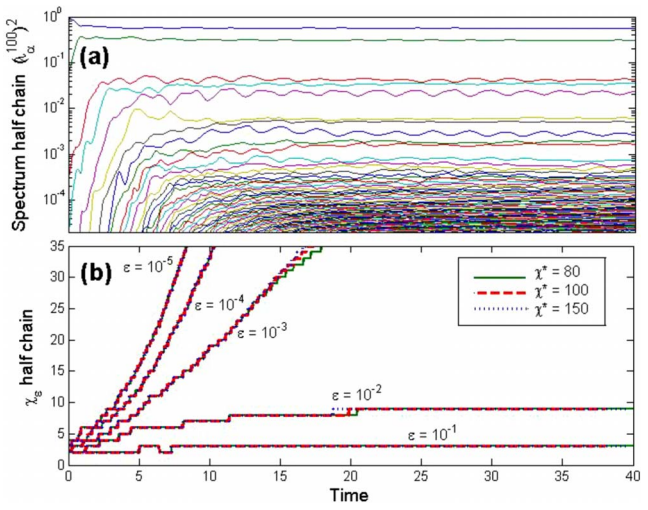

FIG. 4. (Color online) Entanglement growth at the center of the chain for the Ising model with tilted magnetic field, Eq. (6), in the same scenario as Fig. 3. (a) As in Fig. 2(a), starting from a barely entangled state, with only a few nonvanishing Schmidt coefficients, several other coefficients start to grow, then tend to saturate; (b) but while rank χ_ϵ still saturates for $\epsilon=0.1,0.01$, it keeps growing (approximately linearly) for lower values $\epsilon=10^{-3},10^{-4}$. [Notice that we have superposed the results of simulations performed with a MPS of increasing rank $\chi^*=80,100,150$. The results are generally very similar (except, e.g., for a small variation in $\chi_{\epsilon=10^{-3}}$)].

Although the scaling of χ_ϵ described in this paper corresponds to *large* times in a *large* system, both the time and the system size are obviously finite. Our results show that at least during a valuably large period of time, the entanglement grows in a moderate way, enabling the efficient, accurate simulation of the evolution. Whether at even larger times the simulation remains efficient is hard to tell. This is not too relevant, however, in all those applications where the interesting phenomena occur within moderate times from the moment the perturbation is introduced.

In conclusion, we have studied the generation of entanglement in a particularly relevant class of time evolutions, namely those that follow from locally perturbing the ground state of a system, which are related to the computation of unequal-time two-point correlators (2) in one spatial dimension. Our results provide strong evidence that such evolutions can quite often be efficiently simulated with algorithms, such as the TEBD, based on updating a MPS [2,3,5–8]. Our expectation is that the scaling of entanglement that we have observed for the specific models under consideration also applies to most one-dimensional models of interest in condensed matter physics and quantum statistical mechanics. It would be extremely interesting to be able to formally justify these results. This does not seem to be an easy task.

We conclude by describing two simple toy model evolutions that reproduce the two observed patterns of entangle-

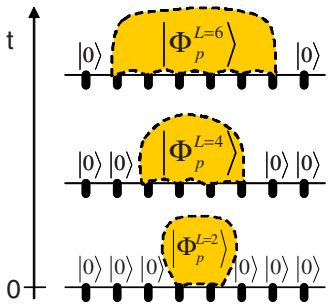

FIG. 5. (Color online) Toy model for the time evolutions of examples I and II of Sec. III. The chain is initially in a ground state with all spins in state $|0\rangle$. Either 1 or 2 spins are flipped into state $|1\rangle$ at the middle of the chain, and the evolution produces an entangled state $|\Phi_p^L\rangle$ of Eqs. (11) and (12) ($p=1$ or 2) that involves a number L of central spins that grows linearly in time.

ment scaling. Initially, a spin chain is in a ground state where all the spins are in state $|0\rangle$. In one case, the perturbation flips one single spin into state $|1\rangle$, and the time evolution produces an entangled state

$$|\Phi_1^L\rangle \equiv \frac{1}{\sqrt{L}} \sum_i |0_1 \cdots 1_i \cdots 0_L\rangle \tag{11}$$

involving the L central spins of the chain, where L grows linearly in time, $L=2vt$, with v the speed of propagation of the perturbation; see Fig. 5. Here, $|\Phi_1^L\rangle$ is a linear combination of all the strings of L spins containing one single one. It can be seen that in any link of the chain, the Schmidt rank χ will go from 1 (before the expanding perturbation has reached that link) to just 2. Thus this model reproduces the saturation observed in example I. In the second case, the perturbation flips two spins into state $|1\rangle$ and the time evolution produces an entangled state

$$|\Phi_2^L\rangle \equiv \frac{1}{\sqrt{L(L-1)}} \sum_{i,j\neq i} |0_1 \cdots 1_i \cdots 1_j \cdots 0_L\rangle \tag{12}$$

involving the L central spins of the chain, where as before L grows linearly in time, $L=2vt$. Now $|\Phi_2^L\rangle$ is a linear combination of all the strings of L spins containing two ones. It can be seen that in any link of the chain, the Schmidt rank χ grows linearly in time from the moment the expanding perturbation reaches that link. Therefore this second evolution reproduces the moderate steady growth observed in example II. Perhaps then (more sophisticated versions of) these toy models will inspire new simulation algorithms, based on an alternative ansatz that is even more efficient than a MPS for the considered class of time evolution.

ACKNOWLEDGMENTS

A.P. thanks A. Doherty for his hospitality at the University of Queensland and acknowledges financial support from the Spanish MEC (Programa para la Movilidad) and from the Universidad de Alcalá (Ayudas a la Movilidad). G.V. acknowledges financial support from the Australian Research Council (Grant Nos. FF0668731 and DP0878830).

[1] S. R. White, Phys. Rev. Lett. **69**, 2863 (1992); Phys. Rev. B **48**, 10345 (1993).
[2] G. Vidal, Phys. Rev. Lett. **91**, 147902 (2003).
[3] G. Vidal, Phys. Rev. Lett. **93**, 040502 (2004).
[4] M. Fannes *et al.*, Commun. Math. Phys. **144**, 443 (1992); S. Ostlund and S. Rommer, Phys. Rev. Lett. **75**, 3537 (1995).
[5] F. Verstraete, J. J. Garcia-Ripoll, and J. I. Cirac, Phys. Rev. Lett. **93**, 207204 (2004); M. Zwolak and G. Vidal, *ibid.* **93**, 207205 (2004); J. J. Garcia-Ripoll, New J. Phys. **8**, 305 (2006).
[6] S. R. White and A. E. Feiguin, Phys. Rev. Lett. **93**, 076401 (2004).
[7] A. J. Daley *et al.*, J. Stat. Mech.: Theory Exp. (2004) P04005.
[8] U. Schollwöck and S. R. White, in *Effective Models for Low-dimensional Strongly Correlated Systems*, edited by G. G. Batrouni and D. Poilblanc (AIP, Melville, NY, 2006), p. 155; e-print arXiv:cond-mat/0606018v1.
[9] L. Amico, A. Osterloh, F. Plastina, R. Fazio, and G. M. Palma, Phys. Rev. A **69**, 022304 (2004); T. S. Cubitt and J. I. Cirac, e-print arXiv:quant-ph/0701053v1.
[10] R. Jozsa and N. Linden, e-print arXiv:quant-ph/0201143.
[11] T. J. Osborne, Phys. Rev. Lett. **97**, 157202 (2006).
[12] P. Calabrese and J. L. Cardy, J. Stat. Mech.: Theory Exp. (2007) P10004.
[13] V. Eisler and I. Peschel, J. Stat. Mech.: Theory Exp. (2007) P06005; V. Eisler, D. Karevski, T. Platini, and I. Peschel, *ibid.* (2008) P01023.
[14] A. Kleine, C. Kollath, I. P. McCulloch, T. Giamarchi, and U. Schollwock, Phys. Rev. A **77**, 013607 (2008).
[15] G. L. Giorgi and F. de Pasquale, Phys. Rev. A **78**, 022305 (2008).
[16] D. Gobert, C. Kollath, U. Schollwock, and G. Schutz, Phys. Rev. E **71**, 036102 (2005).
[17] G. De Chiara, S. Montangero, P. Calabrese, and R. Fazio, J. Stat. Mech.: Theory Exp. (2006), P03001.
[18] C. K. Burrell and T. J. Osborne, Phys. Rev. Lett. **99**, 167201 (2007).
[19] T. Prosen and M. Znidaric, Phys. Rev. E **75**, 015202(R) (2007).
[20] The truncation error refers to the whole state of the chain. The induced (relative) errors in the expectation value of a local observable are often up to several orders of magnitude smaller than ϵ.
[21] As a (finite size) model approaches a quantum critical point, its ground state displays more and more entanglement. Consequently, a larger χ_ϵ is required in order to achieve the same accuracy ϵ. However, the scaling of χ_ϵ with time still seems to follow the same patterns as in the noncritical case.
[22] A. T. Sornborger and E. D. Stewart, Phys. Rev. A **60**, 1956 (1999).